environmental microbiology

Environmental Microbiology (2016) **18**(9), 3159–3174 doi:10.1111/1462-2920.13387

Anaerobic microbial Fe(II) oxidation and Fe(III) reduction in coastal marine sediments controlled by organic carbon content

Katja Laufer,[1] James M. Byrne,[1] Clemens Glombitza,[2] Caroline Schmidt,[1] Bo Barker Jørgensen[2] and Andreas Kappler[1,2*]

[1]*Geomicrobiology, Center for Applied Geosciences, University of Tuebingen, Tuebingen, Germany.*

[2]*Department of Bioscience, Center for Geomicrobiology, Aarhus University, Aarhus, Denmark.*

Summary

Coastal marine sediments contain varying concentrations of iron, oxygen, nitrate and organic carbon. It is unknown how organic carbon content influences the activity of nitrate-reducing and phototrophic Fe(II)-oxidizers and microbial Fe-redox cycling in such sediments. Therefore, microcosms were prepared with two coastal marine sediments (Kalø Vig and Norsminde Fjord at Aarhus Bay, Denmark) varying in TOC from 0.4 to 3.0 wt%. The microcosms were incubated under light/dark conditions with/without addition of nitrate and/or Fe(II). Although most probable number (MPN) counts of phototrophic Fe(II)-oxidizers were five times lower in the low-TOC sediment, phototrophic Fe(II) oxidation rates were higher compared with the high-TOC sediment. Fe(III)-amended microcosms showed that this lower net Fe(II) oxidation in the high-TOC sediment is caused by concurrent bacterial Fe(III) reduction. In contrast, MPN counts of nitrate-reducing Fe(II)-oxidizers and net rates of nitrate-reducing Fe(II) oxidation were comparable in low- and high-TOC sediments. However, the ratio of $nitrate_{reduced}$:$iron(II)_{oxidized}$ was higher in the high-TOC sediment, suggesting that a part of the nitrate was reduced by mixotrophic nitrate-reducing Fe(II)-oxidizers and chemoorganoheterotrophic nitrate-reducers. Our results demonstrate that dynamic microbial Fe cycling occurs in these sediments and that the extent of Fe cycling is dependent on organic carbon content.

Received 27 February 2016; revised 18 May 2016; accepted 20 May 2016. *For correspondence. E-mail andreas.kappler@uni-tuebingen.de; Tel. +49-7071-2974992; Fax: +49-7071-29-295059.

Introduction

Iron is an abundant redox-active element in sediments (Canfield *et al.*, 1993a) and is important for both biotic and abiotic redox processes. Fe can occur in a wide range of redox states from −II to +VI. The major redox states of Fe in the environment are Fe(II) (ferrous iron) and Fe(III) (ferric iron). In marine sediments, Fe is present mainly in the form of iron sulfides, as poorly crystalline Fe(III) (oxyhydr)-oxides or in silicates (Canfield, 1989; Canfield *et al.*, 1993a,b; Moeslund *et al.*, 1994; Haese, 2006). Concentrations of dissolved Fe(II), i.e. Fe^{2+}_{aq}, in sediment porewater usually range from a few to a few hundred μM (Thamdrup *et al.*, 1994).

Under anoxic conditions at circumneutral pH, the conversion of Fe(II) to Fe(III) and *vice versa* can be mediated by different abiotic and biotic processes (Melton *et al.*, 2014a). Abiotic reactions include Fe(III) reduction by e.g. reduced sulfur species or organics such as humic substances and Fe(II) oxidation by Mn(IV) oxides or reactive nitrogen species, for example NO_2^- or NO.

Several microbial processes are involved in Fe redox cycling under anoxic conditions (Weber *et al.*, 2006a; Melton *et al.*, 2014a). On the reductive side of the microbial Fe cycle there are bacteria that reduce Fe(III) while oxidizing organic carbon or hydrogen (Lovley, 1991). On the oxidative side, anaerobic microbial Fe(II) oxidation can be performed either by nitrate-reducing Fe(II)-oxidizing bacteria (Straub *et al.*, 1996), or by anoxygenic phototrophic Fe(II)-oxidizing bacteria, the so-called photoferrotrophs (Widdel *et al.*, 1993). Whereas for the photoferrotrophs it has been unambiguously shown that many strains can live photolithoautotrophically by Fe(II) oxidation, there is still some debate regarding the nitrate-reducing Fe(II)-oxidizers. It remains unknown whether some of these organisms can live chemolithoautotrophically by oxidizing Fe(II) enzymatically coupled to CO_2 and nitrate reduction (in the following called autotrophic Fe(II)-oxidizing nitrate-reducers). It is also possible that the Fe(II) oxidation observed during microbial nitrate reduction is an abiotic side-reaction caused by reactive N-intermediates such as NO_2^- stemming either from chemoorganoheterotrophic nitrate reduction (in the following called heterotrophic nitrate

reduction) or from mixotrophic processes, i.e. using both organic and inorganic carbon compounds as carbon source (Klueglein and Kappler, 2012; Carlson *et al.*, 2013; Chakraborty and Picardal, 2013; Klueglein *et al.*, 2014; 2015). Even if Fe(II) oxidation is an abiotic reaction initiated by nitrite produced during denitrification, it is likely to still be an environmentally relevant process. Chakraborty and colleagues (2011), Muehe and colleagues (2009), and Benz and colleagues (1998) showed that the addition of Fe(II) stimulates cellular growth yields at both environmentally relevant Fe(II), acetate, and nitrate concentrations (in the μM range) and at concentrations commonly used for laboratory cultivation (in the mM range), suggesting that bacteria are benefitting and probably even gaining energy from Fe(II) oxidation under these conditions.

These different biotic and abiotic Fe redox reactions cause the precipitation, transformation, and dissolution of different minerals and the biogeochemical Fe cycle is connected to many other elementary cycles, e.g. the carbon, nitrogen, sulfur and phosphorous cycle (Canfield, 1989; Martin *et al.*, 1991; Widdel *et al.*, 1993; Straub *et al.*, 1996; Emerson and Moyer, 1997; Boyd *et al.*, 2007). In nature Fe(II)-oxidizing and Fe(III)-reducing bacteria can be found in close proximity to each other, especially when biogeochemical gradients are steep e.g. in lake sediments, river floodplain sediments, groundwater, soil and in marine coastal sediments (Coby *et al.*, 2011; Melton *et al.*, 2012; Shelobolina *et al.*, 2012; Benzine *et al.*, 2013; Laufer *et al.*, 2016). Fe(III) minerals produced by nitrate-reducing Fe(II)-oxidizers are a suitable substrate for microbial Fe(III) reduction (Straub *et al.*, 1998; Straub *et al.*, 2004). There have been several studies of Fe-cycling by nitrate-reducing Fe(II)-oxidizers, phototrophic Fe(II)-oxidizers and Fe(III)-reducers in freshwater environments, groundwater habitats, and even in pure-culture experiments where the redox-active mineral magnetite was used as an electron donor and acceptor (Straub *et al.*, 2004; Weber *et al.*, 2006b; Coby *et al.*, 2011; Melton *et al.*, 2012; Shelobolina *et al.*, 2012; Benzine *et al.*, 2013; Byrne *et al.*, 2015).

Based on measured Fe reduction rates, Canfield and colleagues (1993b) estimated that in marine sediments an Fe atom is cycled up to 300 times by an interplay of aerobic and anaerobic processes before it is finally buried in the sediment. In contrast to freshwater sediments, where Fe(III) reduction is often the prevailing pathway for anaerobic organic matter degradation, sulfate reduction is usually more important in marine sediments. However, there are also marine shelf sediments where Fe(III) reduction contributes up to 50% to organic matter mineralization (Thamdrup, 2000), and in deep-sea sediments metal reduction can even be the most important anaerobic mineralization pathway (D' Hondt *et al.*, 2004). Despite this existing knowledge about the potential presence of Fe redox cycling in marine sediments, there is little information about the rates of microbial Fe(II) oxidation under varying geochemical conditions in such environments, especially where microbial Fe(II) oxidation could be an important source of oxidized Fe for Fe(III)-reducing bacteria.

In a recent study (Laufer *et al.*, 2016), we have shown that nitrate-reducing Fe(II)-oxidizers, photoferrotrophs and Fe(III)-reducers co-exist in the same layers of two geochemically distinct but widely representative marine sediments. In the present study, we evaluate the potential activity of anaerobic Fe(II)-oxidizers in the same two coastal marine sediments, i.e. in organic-rich estuarine sediment from Norsminde Fjord (Denmark) and in organic-poor sediment from a sandy beach in Kalø Vig (Denmark). The objectives of this study were to determine potential rates of anaerobic Fe(II) oxidation by photoferrotrophs and nitrate-reducing Fe(II)-oxidizers in microcosms with the two sediments. By conducting experiments with added Fe(III), we aimed to identify concurrent processes of microbial Fe redox cycling in the organic-rich sediment. Additionally, we quantified dissolved organic carbon (DOC) and volatile fatty acid (VFA) concentrations to understand the combined influence of organic carbon on microbial Fe(II) oxidation and Fe(III) reduction.

Results

Geochemical measurements – sediment and porewater characteristics

The sediments from Norsminde Fjord and Kalø Vig were distinctly different based on visual observations and geochemical analyses. The Norsminde Fjord sediment was fine grained and muddy. In June 2014, the upper ca. 0.5 cm was oxidized as indicated by a light-brown colour while below 0.5 cm the sediment was blackish. In February 2015 the light-brown layer was 1 cm thick. The Kalø Vig sediment had a coarser grain size. In June 2014, the upper 0–2 mm were light-brown, below which a 1–2 mm purple layer was observed, probably containing anoxygenic phototrophic bacteria, followed by a darker greyish layer. In February 2015, the Kalø Vig sediment was light-brown in the top 0–1 cm and was greyish below that. The results of the geochemical analyses for both field sites are presented in Table 1. The Norsminde Fjord and Kalø Vig sediments will be referred to as high-TOC and low-TOC respectively.

Phototrophic iron(II) oxidation in high-TOC and low-TOC sediment

In order to evaluate the potential for phototrophic Fe(II) oxidation, we quantified total Fe(II) and Fe(III) in light-incubated microcosms, (i) without amendments in the high-TOC sediment and (ii) amended with Fe(II) in both

Table 1. Geochemical data of sediment from Norsminde Fjord (high-TOC) and Kalø Vig (low-TOC) that was sampled in June 2014 and February 2015.

Parameter	High-TOC		Low-TOC	
	June 14	February 15	June 14	February 15
Sediment water content (wt. %)	71% ± 3%	69% ± 4%	19% ± 4%	22% ± 2%
Salinity	17.7	23.6	22.4	23.3
DOC water column	5.3 ± 0.1 mg l^{-1}	5.4 ± 0.1 mg l^{-1}	4.2 ± 0.1 mg l^{-1}	4.4 ± 0.1 mg l^{-1}
DOC porewater [a]	8.2 ± 0.1 mg l^{-1}	5.1 ± 0.2 mg l^{-1}	6.6 ± 0.1 mg l^{-1}	5.6 ± 0.1 mg l^{-1}
TOC sediment [a]	3.31% ± 0.4%	2.98% ± 0.2%	0.38% ± 0.05%	0.45% ± 0.32%
VFA in porewater [a]	17.8 ± 3.7 μM	N.D.	26.6 ± 2.8 μM	N.D.
NO_3^- porewater [a]	18.3 ± 8.2 μM	20.3 ± 5.3 μM	4.2 ± 2.4 μM	11.6 ± 2.9 μM
NO_2^- porewater[a]	Bdl	Bdl	Bdl	Bdl
pH water column	7.9	7.9	8.1	7.8
pH anoxic porewater [sediment depth]	7.1 [4 mm]	7.0 [5 mm]	6.9 [4 mm]	7.2 [7 mm]
O_2 sat.water column	100%	100%	100%	100%
O_2 penetr. depth in sediment	1.5 mm	3.5 mm	2 mm	5 mm
Light penetr. depth in sediment	2.0 mm	N.D.	2.9 mm	N.D.
Redox potential at sediment surface	+256 mV	+490 mV	+284 mV	+435 mV
Redox potential in anoxic sediment [sediment depth]	−85 mV [4 mm]	−77 mV [20 mm]	−75 mV [4 mm]	+263 mV [15 mm]
Sulfide in porewater[b]	18.5 ± 4.2 μM	Bdl	757 ± 68 μM	47 ± 23 μM
Fe(II) in porewater[a]	104 ± 64 μM	82 ± 73 μM	70 ± 52 μM	23 ± 53 μM
Fe(II) in solid phase[a] (1 M HCl extract)	89 ± 52 μmol g^{-1} dw	92 ± 36 μmol g^{-1} dw	8 ± 2 μmol g^{-1} dw	0.4 ± 0.1 μmol g^{-1} dw
Fe(II)/Fe(III) ratio in solid[a] phase (1 M HCl extract)	3.05	3.26	3.37	2.89

a. Mean value for measurements in the upper 3 cm of the sediment.
b. Maximum concentration that was measured in the upper 2 cm of the sediment.
N.D., not determined; bdl, below detection level.

the high-TOC and low-TOC sediment over time. We found that Fe(II) was oxidized in the light in all incubations with higher rates in the low-TOC sediment (Figs. 1A and 2A; Table 2). By placing previously light incubated high-TOC sediment in the dark (Fig. 1B), or by adding Fe(III) to light incubated high-TOC sediment (Fig. 3A), we found high activity of Fe(III)-reducing bacteria, which explains the lower net phototrophic Fe(II) oxidation rates (see data in Table 2). In the NaN_3-treated controls for both sediments, Fe(II) or Fe(III) did not change over time.

When Fe(III) was added to light incubated high-TOC sediment, we found that during the first 28 days Fe(III) reduction was prevailing, indicated by increasing Fe(II) concentrations (Fig. 3A). Subsequently, there was a phase of 15 days where Fe(II) concentrations remained constant, followed by a phase where Fe(II) was decreasing indicating Fe(II) oxidation (Fig. 3A). The calculated rates of Fe(II) oxidation and Fe(III) reduction, and the lengths of the different phases, are shown in Table 2.

To confirm that the observed Fe(II) oxidation in light was caused by anoxygenic phototrophic Fe(II)-oxidizers, and not by oxidation with O_2 produced by oxygenic phototrophs, we repeated the experiments with both sediments using infra-red (IR) light-pass filters to exclude wavelengths used by oxygenic phototrophs. We found similar Fe(II) oxidation rates with and without filters, suggesting that the observed Fe(II) oxidation was caused by anoxygenic phototrophs (Supporting Information Fig. S1; Table 2).

Nitrate-reducing iron(II) oxidation in high- and low-TOC sediment

In order to evaluate the potential for nitrate-reducing Fe(II) oxidation, we quantified Fe(II), Fe(III), NO_3^- and NO_2^- in experiments amended with (i) NO_3^- in high-TOC sediment and (ii) NO_3^- and Fe(II) in both high- and low-TOC sediment. During dark incubation, we found that in both sediments, Fe(II) was oxidized at similar rates (Figs. 2 and 4; Table 2), but with different stoichiometry of $nitrate_{reduced}$:$Fe(II)_{oxidized}$ (Table 2) indicating a higher contribution of heterotrophic nitrate reduction in the high-TOC sediment. In this sediment type, the activity of Fe(III)-reducers continued after NO_3^-

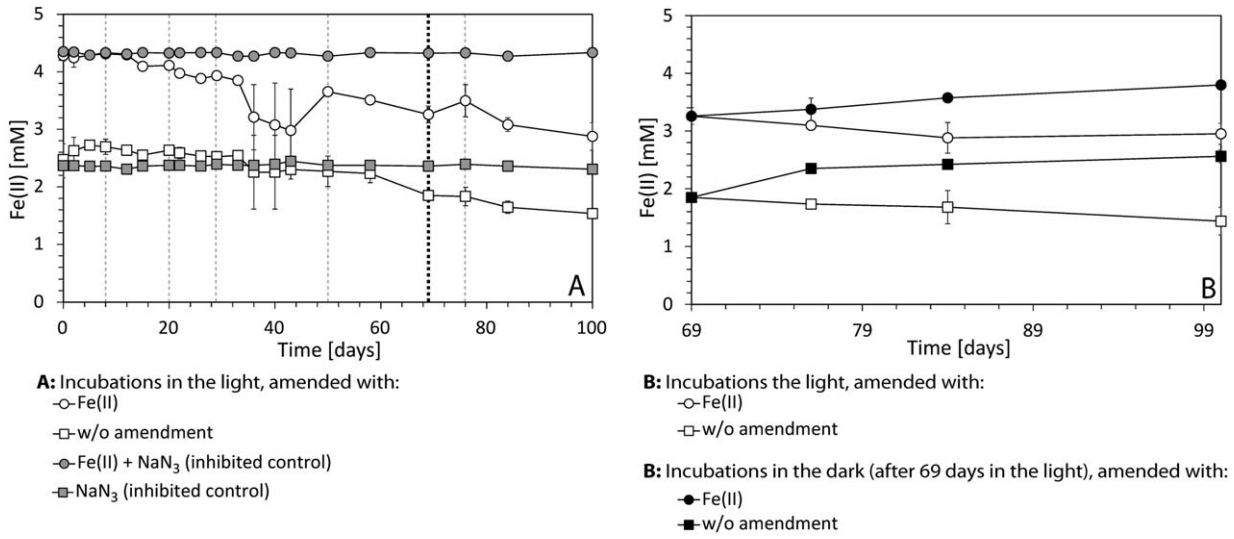

Fig. 1. Fe(II) concentrations over time in high-TOC sediment (June 2014).
A. Incubation in the light. Vertical dashed lines indicate time points of triplicate analyses.
B. After 69 days in the light (bold black vertical dashed line in A), new triplicate microcosms remained in the light or were transferred to the dark. The increase in Fe(II) in the dark shows a concurrent Fe(III) reduction to Fe(II). This Fe(III) reduction counteracts the Fe(II) oxidation in the light. Error bars show standard deviation of triplicates (in some cases smaller than symbol size).

was consumed (Figs. 3 and 4). The re-addition of NO_3^- or ferrihydrite to the high-TOC sediment after 47 days of incubation stimulated the activity of nitrate-reducing Fe(II)-oxidizers and Fe(III)-reducers, respectively, (Fig. 4).

In order to quantify the effect of the initial addition of Fe(III) on Fe-cycling in the high-TOC sediment, microcosms were amended with 4 mM NO_3^-, 2 mM Fe(II) and 2 mM Fe(III). Similar to the previous experiments we found initial Fe(II) oxidation and simultaneous nitrate reduction (Fig. 3). When nitrate was completely consumed, Fe(III) was reduced again to Fe(II) (Fig. 3). The rates of Fe(II) oxidation and the stoichiometry of $nitrate_{reduced}$:$Fe(II)_{oxidized}$ were lower compared with the previous high TOC microcosms (Table 2).

Activity of Fe(III)-reducing bacteria in the high-TOC sediment

Several microcosms that were set up with high-TOC sediment showed evidence for microbial Fe(III) reduction.

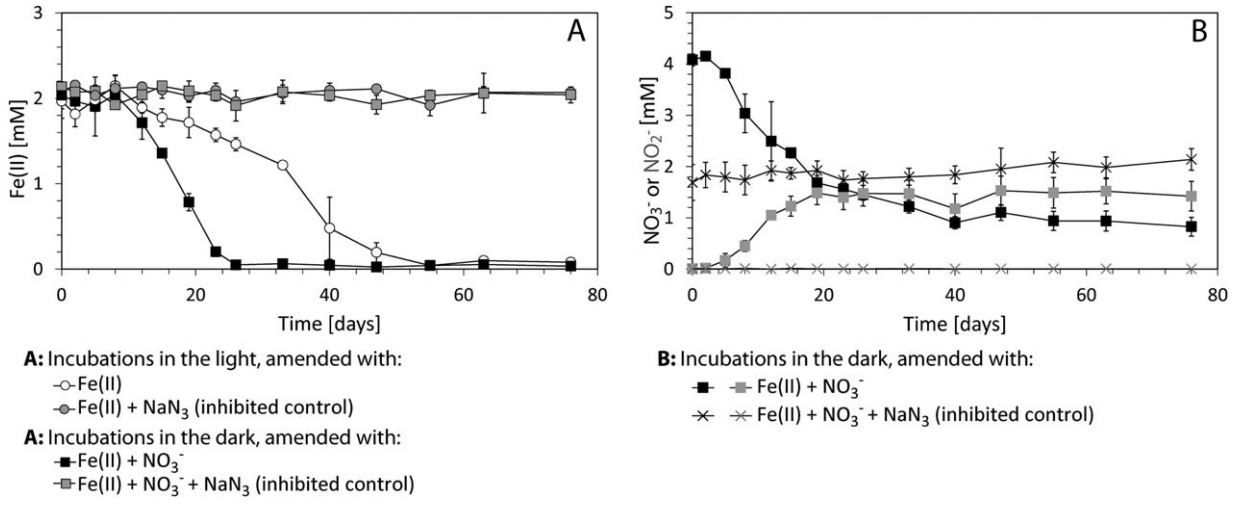

Fig. 2. Fe(II) oxidation and NO_3^- reduction over time in low-TOC sediment (June 2014).
A. Fe(II) concentrations over time.
B. NO_3^- (black symbols) and NO_2^- (grey symbols) concentrations over time. Error bars show standard deviation of triplicates (in some cases smaller than symbol size).

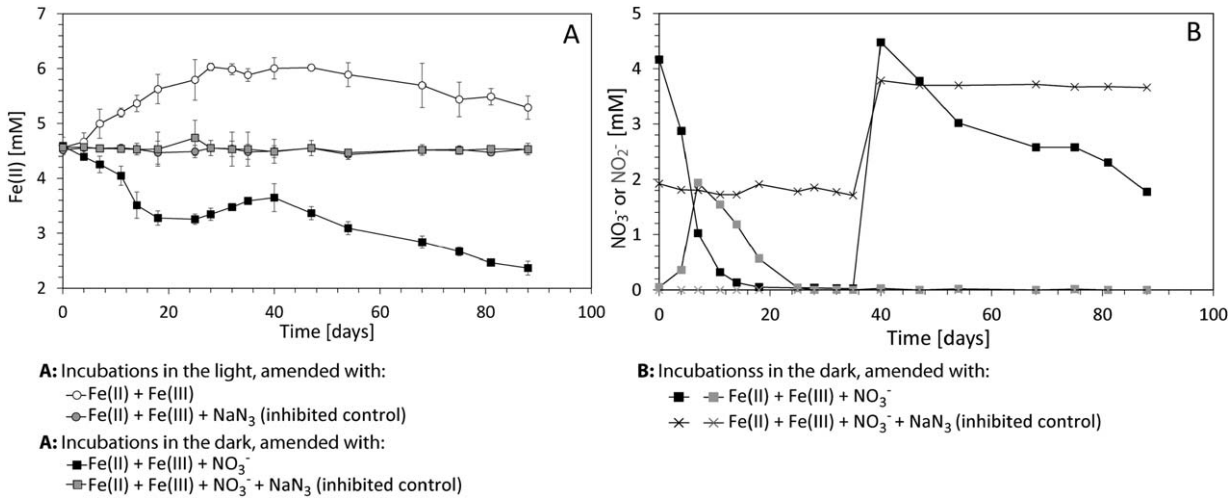

Fig. 3. Iron-cycling and NO_3^- reduction over time in Fe(III) + Fe(II) amended high-TOC sediment (February 2015).
A. Fe(II) concentrations over time.
B. NO_3^- (black symbols) and NO_2^- (grey symbols) concentrations over time. A+B: After 40 days NO_3^- was re-added to dark incubated sediment, what led to further Fe(II) oxidation. Error bars show standard deviation of triplicates (in some cases smaller than symbol size).

Specifically, we found Fe(II) formation in (i) dark-incubated microcosms after NO_3^- was used up (Figs. 3 and 4), (ii) in non-amended or Fe(II)-amended microcosms that were shifted from light to dark conditions (Fig. 1B), (iii) in dark incubated microcosms to which Fe(III) was added (Figs. 3 and 4C) and (iv) in microcosms that were incubated in the light where initially Fe(II) and Fe(III) were added (Fig. 3). Fe(III) reduction rates were highest in the high-TOC sediment sampled in June 2014 after NO_3^- was consumed during the first Fe-redox cycle (Table 2). Lowest Fe(III) reduction rates were found in the high-TOC sediment when previously light-incubated microcosms where shifted into the dark (Table 2).

Development of organic carbon concentrations (VFA and DOC) in high-TOC sediment

In order to link microbial Fe(II) oxidation and Fe(III) reduction processes to the C-cycle and to the bioavailability of organic carbon, changes in DOC and VFA concentrations were followed over time in dark- and light-incubated microcosms with high-TOC sediment. The corresponding Fe(II) and NO_3^- concentrations in the respective microcosms are shown in Figs. 1 and 4. The bulk concentration of all VFAs (formate, acetate, propionate, butyrate, iso-butyrate, valerate, pyruvate, lactate, iso-valerate) in the microcosms was 31.5 ± 2.5 μM (Fig. 5).

In general, VFA concentrations decreased when Fe(II) was oxidized and nitrate was reduced, while they increased when Fe(III) was reduced. The lowest concentrations (0.8 ± 0.7 μM) were found in the microcosms that were incubated for 5 days in the dark with NO_3^- amendment (Fig. 5). Maximum VFA concentrations of 332.4 ± 31.1 μM were reached after 100 days of incubation in those microcosms that were shifted after 69 days from light to dark. In non-amended microcosms that were incubated in the dark, as well as in the NaN_3 treated controls VFA concentrations increased during incubation. They accumulated to 414.8 ± 57.6 μM and 436.8 ± 25.2 μM after 100 days, respectively, (Fig. 5; Supporting Information Fig. S2). In all cases, the largest variations were found for acetate where concentrations varied from below detection limit (0.2 μM) and 435 μM throughout the incubation. In most cases the other VFA concentrations followed the general trends that can be seen in Fig. 5 but the relative variations were much smaller than for acetate (Supporting Information Fig. S2).

In non-amended microcosms incubated for 69 days in light followed by 31 days in the dark, the concentrations of DOC increased over time, from 6.3 ± 0.4 mg l^{-1} to 25.6 ± 1.2 mg l^{-1} (Table 3). In non-amended microcosms that were only incubated in the dark throughout the 100 days of incubation, DOC concentrations increased to 20.16 ± 1.3 mg l^{-1} (Table 3). The increase in DOC was more pronounced when Fe(III) reduction was active in the microcosms, i.e. when previously light-incubated microcosms were placed in the dark or in dark-incubated microcosms when nitrate was depleted (Table 3).

Most probable numbers of Fe-metabolizing microorganisms

Freshly sampled high-TOC sediment (collected in June 2014) contained 4.4×10^2 cells g^{-1} dry weight (dw) of phototerrotrophs, and 4.0×10^3 and 3.1×10^3 cells g^{-1} dw of nitrate-reducing Fe(II)-oxidizers in most probable number

Table 2. Calculated stoichiometries and rates for the microcosm experiments. A: Changes of the stoichiometry of $nitrate_{reduced}$:$iron(II)_{oxidized}$ in different microcosms with high-TOC and low-TOC sediment. B: Maximum rates of Fe(II) oxidation. C: maximum rates of Fe(III) reduction. Cycles correspond to oxidation-reduction cycles of Fe in the respective microcosms i.e. the start of the second cycle was when NO_3^- was re-added after the initially added NO_3^- was consumed and Fe(III) was reduced.

A: Microcosm	Cycle (days)	$Nitrate_{reduced}$:$iron(II)_{oxidized}$
High-TOC (June 2014) + NO_3^-	1 (0–15)	4.27
	2 (47–58)	1.25
High-TOC (June 2014)+ Fe(II) + NO_3^-	1 (0–15)	3.04
	2 (47–76)	0.93
Low-TOC (June 2014) + Fe(II) + NO_3^-	1 (8–26)	1.32
High-TOC (Feb. 2015) + Fe(II) + Fe(III) + NO_3^-	1 (0–18)	3.18
	2 (40–88)	1.63
B: Microcosm	Cycle (days)	Fe(II) oxidation [$\mu M\ day^{-1}$][a] (lag phase)
High-TOC (June 2014) light	(33–100)	12 (33 days)
High-TOC (June 2014) light + Fe(II)	(12–100)	19 (12 days)
High-TOC (Feb. 2015) light + Fe(II) + Fe(III)	(47–88)	19 (47 days)
High-TOC (Feb. 2015) IR light + Fe(II)	(22–75)	22 (22 days)
High-TOC (Feb. 2015) light + Fe(II)	(22–75)	15 (22 days)
Low-TOC (June 2014) light + Fe(II)	(8–55)	42 (8 days)
Low-TOC (Feb. 2015) light + Fe(II)	(0–75)	31 (0 days)
Low-TOC (Feb. 2015) IR light + Fe(II)	(0–75)	29 (0 days)
High-TOC (June 2014) + NO_3^-	1 (0–15)	52 (0 days)
	2 (47–58)	141 (0 days)
High-TOC (June 2014) + Fe(II) + NO_3^-	1 (0–15)	124 (0 days)
	2 (47–76)	149 (0 days)
High-TOC (Feb. 2015) + Fe(II) + Fe(III) + NO_3^-	1 (0–18)	71 (0 days)
	2 (40–88)	27 (0 days)
Low-TOC (June 2014) + Fe(II) + NO_3^-	1 (8–26)	111 (8 days)
C: Microcosm	Cycle (days)	Fe(III) reduction [$\mu M\ day^{-1}$][a]
High-TOC (June 2014) + NO_3^-	1 (15–47)	59
	2 (47–100)	48
High-TOC (June 2014) + Fe(II) + NO_3^-	1 (15–47)	59
	2 (47–100)	48
High-TOC (June 2014) L → D	1 (69–100)	23
High-TOC (June 2014) + Fe(II) L → D	1 (69–100)	18
High-TOC (February 2015) + Fe(II) + Fe(III) + NO_3^-	1 (18–40)	27
High-TOC (February 2015) light + Fe(II) + Fe(III)	1 (0–28)	53

a. Fastest rate calculated from at least 3 points at the steepest point of the curve.

(MPN) enumerations without acetate (for autotrophs) and with acetate (for mixotrophs) respectively. MPNs for Fe(III)-reducers were 2.2×10^3 cells g^{-1} dw (Fig. 6). In the high-TOC sediment collected in February 2015, MPN numbers for the three different physiological types of Fe-metabolizers were similar to the June 2014 data (Supporting Information Table S1).

Cell numbers in low-TOC sediment were generally lower compared with the high-TOC sediment except for nitrate-reducing Fe(II)-oxidizers which occurred in similar abundances. In June 2014, the viable counts were 9.3×10^1 cells g^{-1} dw for photoferrotrophs, 4.5×10^3 cells g^{-1} dw for mixotrophic nitrate-reducing Fe(II)-oxidizers, 4.2×10^3 cells g^{-1} dw for autotrophic nitrate-reducing Fe(II)-oxidizers, and 4.1×10^2 cells g^{-1} dw for Fe(III)-reducing bacteria (Supporting Information Table S1). Cell numbers of the different Fe-metabolizing bacteria in low-TOC sediment from February 2015 were comparable to the cell numbers found in June 2014 (Supporting Information Table S1).

In the high-TOC sediment from June 2014, we also measured abundances of the different Fe-metabolizers after 100 days of incubation in microcosms under different conditions. The corresponding Fe(II) and NO_3^- concentrations in the respective microcosms can be seen in Figs. 1 and 4. In light incubated microcosms with and without the addition of Fe(II), MPNs of photoferrotrophs increased roughly 100-fold (Fig. 6), while in microcosms that were incubated in the dark, MPNs for photoferrotrophs decreased, in some cases even to below the detection limit (Fig. 6). Cell numbers of autotrophic nitrate-reducing Fe(II)-oxidizers remained constant in the different microcosm incubations (Fig. 6). In contrast, MPNs for mixotrophic nitrate-reducing Fe(II) oxidizers increased in all microcosm incubations (Fig. 6). Cell numbers of Fe(III)-reducing bacteria remained relatively constant in most of the microcosms (Fig. 6) except the microcosms that were incubated in the light without additives where Fe(III)-reducers increased approximately 10-fold.

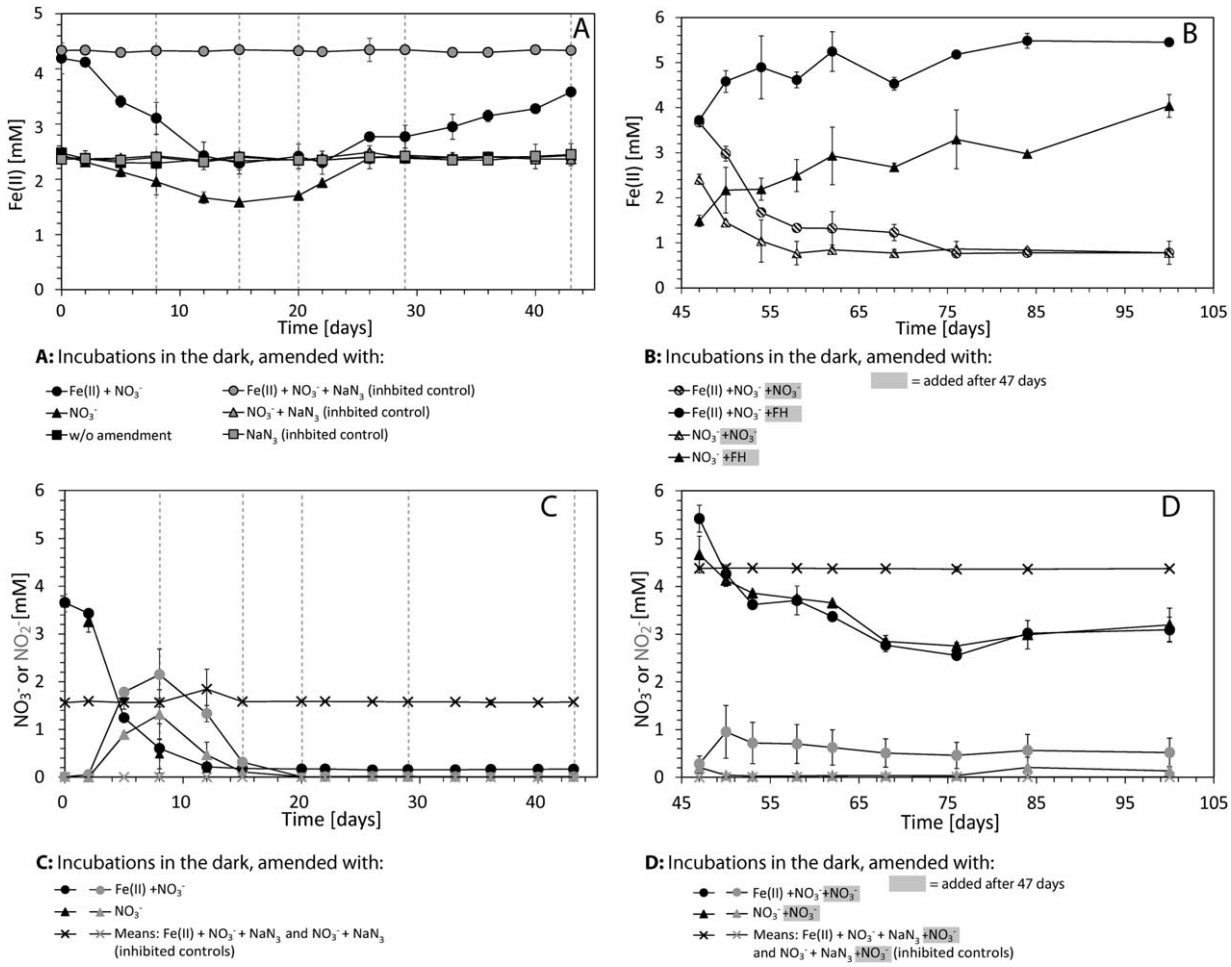

Fig. 4. Fe(II) and NO_3^- concentrations over time in dark incubated high-TOC sediment (June 2014).
A. Fe(II) concentrations over time. The vertical dashed lines indicate when whole microcosm-triplicates were harvested for analysis.
B. Fe(II) over time after re-addition of NO_3^- or Fe(III) at day 47 (the substrate that was re-added, i.e. ferrihydrite or nitrate, is highlighted in the figure legend by grey boxes).
C. NO_3^- (black symbols) and NO_2^- (grey symbols) over time.
D. NO_3^- (black symbols) and NO_2^- (grey symbols) concentrations over time after re-addition. Error bars show standard deviation of triplicates (in some cases smaller than symbol size).

Iron mineralogy in the high-TOC sediment

Mineralogical analysis of the initial high-TOC sediment (Supporting Information Table S2 and Fig. S3) without amendments indicated that it was dominated by Fe(II)/Fe(III) mineral phases that did not undergo magnetic ordering at 5 K. Such behaviour suggests that the iron was present in phyllosilicates (Murad and Cashion, 2004).

Discussion

Abundances of anaerobic Fe(II)-oxidizing and Fe(III)-reducing bacteria

We have previously shown that photoferrotrophs, nitrate-reducing Fe(II)-oxidizers and Fe(III)-reducers co-exist in sediments from Norsminde Fjord (high-TOC) and Kalø Vig (low-TOC) (Laufer *et al.*, 2016). In both the previous and the present study, particularly the initial cell numbers of phototrophic Fe(II)-oxidizers were very low in the sediments with only 10–100 cells g^{-1} dw. However, the MPN method likely underestimates the real number of Fe(II)-oxidizers and Fe(III)-reducers (because usually not all of the present organisms grow in the provided medium) and a quantification based on molecular markers would be necessary to get more accurate cell numbers. Unfortunately, to date no such specific molecular markers for photoferrotrophs or nitrate-reducing Fe(II)-oxidizers are available. Despite the relatively low initial cell numbers in the studied sediments, we could measure significant Fe(II) oxidation under conditions that favor the activity of photoferrotrophs and nitrate-reducing Fe(II)-oxidizers. This clearly demonstrates that the low cell numbers were sufficient to

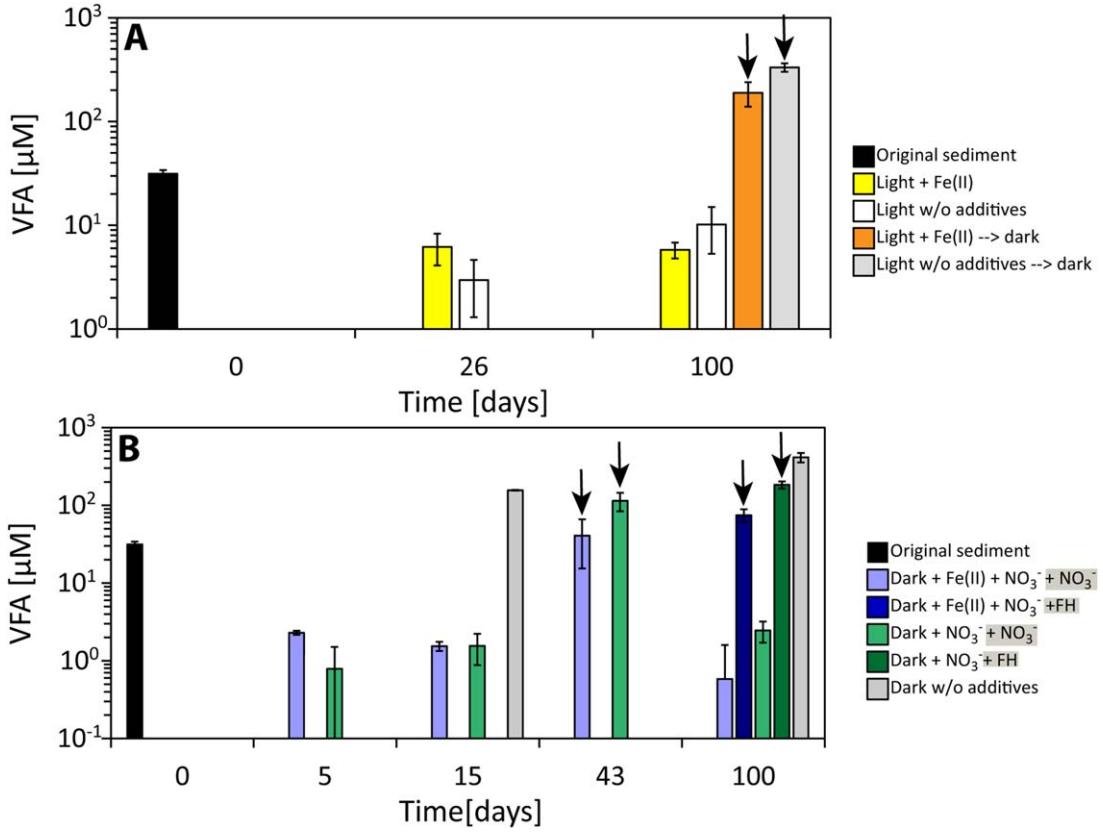

Fig. 5. Development of VFA concentrations (sum of all VFAs) over time in high-TOC sediment (June 2014).
A. Total VFAs in light incubated sediment, except for the orange and the light-grey bars, which show the data for sediment that was shifted to dark incubation after 69 days of incubation in the light.
B. Total VFAs in sediment that was incubated in the dark. The grey boxes in the legend indicate which compound was re-added after 47 days. Arrows mark samples in which Fe(III) reduction was occurring (based on Figure 1 and 4) before measurement of VFA concentrations. Error bars show standard deviation.

accomplish substantial substrate turnover although we observed a prolonged initial lag phase of 10–30 days for phototrophic Fe(II) oxidation. This time, during which no net Fe(II) oxidation was measured, is yet likely explained by the concurrent activity of Fe(III)-reducers. No such lag phase was observed for nitrate-reducing Fe(II)-oxidizers indicating that the addition of nitrate prevented the concurrent activity of Fe(III)-reducers, probably due to

Table 3. Changes in DOC over time in high- and low-TOC sediment (June 2014).

Microcosm	DOC [mg l^{-1}] Start	DOC [mg l^{-1}] after 26 days	DOC [mg l^{-1}] after 43 days	DOC [mg l^{-1}] after 100 days
High-TOC light + Fe(II)	6.3 (±0.4)	N.D.	6.9 (±0.8)	L: 9.1 (±0.7) L→D: 18.9 (±1.5)
High-TOC light w/o add.	6.3 (±0.4)	N.D.	7.01 (±0.8)	L: 8.5 (±0.8) L→D: 25.6 (± 1.2)
High-TOC dark + NO_3^- + Fe(II)	6.3 (±0.4)	6.8 (±1.1)	11.8 (±0.9)	+ NO_3^-: 15.23 (±0.5) ± FH: 23.1 (±0.3)
High-TOC dark + NO_3^-	6.3 (±0.4)	8.1(±0.7)	9.2 (±0.4)	+ NO_3^-: 16.30 (±0.6) ± FH: 21.03 (±1.2)
High-TOC dark w/o add.	6.3 (±0.4)	N.D.	N.D.	20.16 (±1.3)
Low-TOC dark + NO_3^- + Fe(II)	5.11 (±0.5)	N.D.	N.D.	6.78 (±0.3)

Underlined values indicate that Fe(III) reduction was active in these microcosms before DOC was measured. L→D indicates that these samples were placed in the dark after 69 days of incubation in the light. +NO_3^- and + FH indicate that, after 47 days of incubation either NO_3^- or ferrihydrite were re-added.
N.D., not determined.

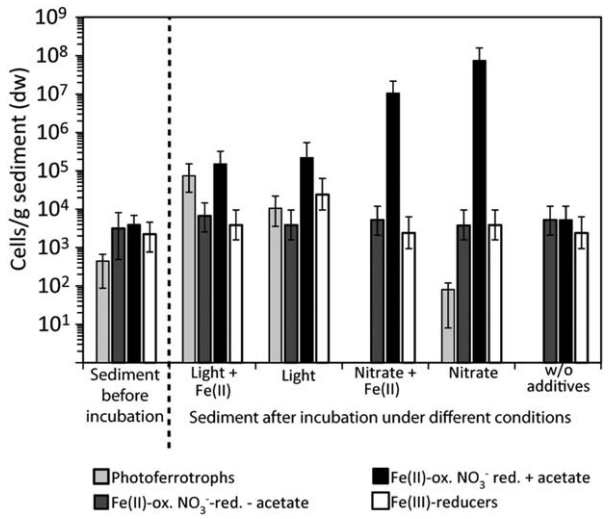

Fig. 6. MPNs of Fe(II)-oxidizers and Fe(III)-reducers before and after incubation of high-TOC sediment (June 2014) in microcosms with different amendments (Fe(II), nitrate) and under different conditions (light/dark). Error bars show standard deviation.

thermodynamic reasons (Sørensen, 1982; Jones *et al*., 1983; Tugel *et al*., 1986). By comparison of the MPNs of Fe-metabolizers in the original sediment with MPNs that were performed after incubation in the microcosms, we found that particularly photoferrotrophs, but also mixotrophic nitrate-reducing Fe(II)-oxidizers, became enriched during the incubation. Cell numbers of autotrophic nitrate-reducing Fe(II)-oxidizers were not increasing during the 100 days of incubation. However, it is likely that in the MPNs from the original sediment we were overestimating the actual numbers of autotrophic nitrate-reducing Fe(II)-oxidizers, because it is likely that mixotrophic nitrate-reducing Fe(II)-oxidizers were also growing in these MPNs due to the high organic carbon content in the sediment. Due to the increasing abundances of phototrophic and nitrate-reducing Fe(II)-oxidizers over time (i.e. an enrichment of these organisms) during microcosm incubation, the Fe(II) oxidation rates determined in the microcosms are, likely overestimating *in situ* Fe(II) oxidation rates in the natural sediment.

Organic carbon degradation in marine sediments – development of DOC and VFA concentrations in microcosm incubations

Although the high-TOC sediment contained about 10 times more TOC than the low-TOC sediment, the initial DOC and VFA concentrations were rather similar. Low sedimentary concentrations of DOC and VFAs indicate that the microorganisms in these sediments are electron donor limited. As a result, DOC and in particular VFAs, once they are produced by hydrolysis and fermentation, are rapidly utilized (Ansbaek and Blackburn, 1980; Christensen and Blackburn, 1982; Parkes *et al*., 1984; Glombitza *et al*., 2014; 2015). This suggests a close connection of fermentation and mineralization of organic matter and explains why the initial DOC and VFA concentrations in the high-TOC and the low-TOC sediments were similar. However, the difference in these two types of sediments is the turnover rate of the organic matter, which is expected to be higher in the high-TOC sediment.

In incubations of the microcosms, DOC and VFA concentrations, particularly acetate, increased with high-TOC sediment during Fe(III) reduction and decreased again during nitrate reduction and Fe(II) oxidation to values even lower than the initial values. Initial VFA concentrations in the microcosms (31.5 ± 2.5 μM) where about 2x higher than the VFA concentrations in the pore water of undisturbed sediment cores (17.8 ± 3.7 μM). This shows that already the mechanical disturbances during preparation of the microcosms influenced the system. The increasing VFA concentrations during Fe(III) reduction indicate a non-balanced carbon budget in the system in which either the VFA production was increased or the VFA consumption was decreased. To evaluate this imbalance, and to roughly estimate the fraction of VFA production that was not consumed during Fe(III) reduction, we did the following calculation. Assuming that Fe(III) reduction was solely fueled by acetate oxidation, with a measured rate of Fe(III) reduction of 59 μM day^{-1} we can calculate that slightly more than 7 μM day^{-1} acetate were oxidized by Fe(III)-reducers (59 μM day^{-1} divided by eight electrons yielded per molecule acetate oxidized). While Fe(III) was reduced at that rate, the concentration of VFAs increased to ca. 40 μM (within 28 days). During these 28 days the Fe(III)-reducers would have oxidized about 196 μM acetate (7 μM day^{-1} acetate multiplied with 28 days). Thus, about 17% of the produced VFAs were not oxidized by Fe(III)-reducers in that case (100% would be the measured 40 μM increase in VFA concentrations plus the 196 μM that were oxidized by Fe(III)-reducers). This is a conservative estimate and the real fraction of the produced VFAs which were not oxidized was probably even higher since the Fe(III)-reducers probably have oxidized other electron donors such as H_2 or other VFAs. Consequently, the high accumulation of acetate during Fe(III) reduction in our microcosms was probably caused by a network of different processes including (i) VFA production by fermenters that exceeded VFA consumption by the Fe(III)-reducers and further fermentation of the VFAs that were not consumed by Fe(III)-reducers to acetate (Schink, 1997; Fuchs, 2007), (ii) consumption of organic electron donors, other than VFAs, by some Fe(III)-reducers and (iii) incomplete oxidation of organic compounds to acetate, including VFAs other than acetate, by some Fe(III)-reducers such as *Shewanella* spp. or *Pelobacter* spp. that are known to oxidize lactate to acetate (Lovley and Phillips, 1989; Caccavo *et al*., 1992; Lovley *et al*., 1995; Rossello-Mora *et al*., 1995).

In previous studies, acetate accumulation during inhibition of sulfate reduction was explained by sulfate-reducers mainly oxidizing acetate. Therefore, acetate was the main VFA accumulating when sulfate-reducers were inhibited (Sørensen *et al.*, 1981; Gibson *et al.*, 1989; Parkes *et al.*, 1989; Fukui *et al.*, 1997; Finke *et al.*, 2007). Similarly, this could mean that in our microcosms, nitrate-reducing bacteria, including mixotrophic nitrate-reducing Fe(II)-oxidizers, mainly use acetate as an electron and carbon source and, therefore, acetate accumulates when nitrate is depleted. However, the organic compounds that accumulated after nitrate was depleted, were not necessarily used by the nitrate-reducers before nitrate depletion. It could also be that the organic compounds that would have been used by nitrate-reducers instead were further metabolized by Fe(III)-reducers or fermenters. For example, as long as nitrate is available, it could be that nitrate-reducers oxidize lactate to CO_2. However, when nitrate is depleted, Fe(III)-reducers or fermenters incompletely oxidize the lactate to acetate. As a consequence, acetate would accumulate although it was not formerly oxidized by nitrate-reducers.

We also found a high accumulation of VFAs, especially acetate, in our NaN_3-treated controls. NaN_3 is an inhibitor of respiratory processes and is specifically inhibiting cytochromes (Wilson and Chance, 1967; Oremland and Capone, 1988), which are not necessary for fermentation. Therefore, fermentation was probably not inhibited in our NaN_3-treated control incubations and fermentation products were accumulating. The maximum accumulation rate of VFAs in the NaN_3 inhibited controls was comparable to the highest values found in the non-NaN_3-treated microcosms. The observation that the accumulation of VFAs was not higher in the NaN_3-treated controls than in the microcosms under Fe(III)-reducing conditions or in the non-amended microcosms that were incubated in the dark could be due to inhibitory effects of the fermentation products (especially H_2) on the activity of the fermenting bacteria preventing a further increase of VFAs (Harper *et al.*, 1986; Fuchs, 2007; Schink and Stams, 2013).

Effect of sediment organic carbon content on photoferrotrophs – why does higher TOC content lead to decreased Fe(II) oxidation by photoferrotrophs?

In microcosms incubated under conditions that favor the activity of photoferrotrophs, we observed Fe(II) oxidation in both sediments but with 1.4–2.2 times higher rates for the low-TOC sediment than for the high-TOC sediment. This was surprising, since the MPN cell numbers for photoferrotrophs were about five times lower in the low-TOC sediment. The higher Fe(II) oxidation rates in the low-TOC sediment could have several explanations: (i) Photoferrotrophs can also live photoheterotrophically and if they prefer organics over Fe(II) (Ehrenreich and Widdel, 1994; Melton *et al.*, 2014c), this explains lower Fe(II) oxidation rates in the high-TOC sediment. (ii) More light reaches the photoferrotrophs in the low-TOC sediment due to the relatively bright quartz sand and large sand particles leading to better light penetration compared with the black mud from the high-TOC sediment. Light penetration depths measured for the high-TOC and the low-TOC sediment were 2 and 2.9 mm, respectively, (Laufer *et al.*, 2016). The total thickness of the sediment layer in the microcosms (at the bottom of the bottles) with high-TOC sediment was about 5 mm and as microcosms were only illuminated from above, only about 40% of the sediment in the high-TOC microcosms was illuminated. In contrast, in the low-TOC sediment the thickness of the sediment layer was only 2–3 mm (due to the lower water content, the 5 g of this sediment had a lower volume than the high-TOC sediment) and consequently almost all of the sediment was illuminated. (iii) In the high-TOC sediment Fe(III) reduction is happening simultaneously with phototrophic Fe(II) oxidation leading to lower net Fe(II) oxidation rates (Fig. 7). Together with the lower light-availability in the high-TOC sediment, the simultaneous activity of Fe(III)-reducers most likely had the largest effect on the measured net Fe(II) oxidation rates. Consequently, we observed substantial Fe(III) reduction occurring in the high-TOC sediment, either when previously light incubated microcosms were shifted to the dark (Fig. 1B, Fe(III) reduction of up to 18–23 $\mu M\ day^{-1}$) or when Fe(III) was added to microcosms even when these microcosms were incubated in the light (Fig. 3A, Fe(III) reduction of up to 53 $\mu M\ day^{-1}$). However, since we observed net Fe(II) oxidation, phototrophic Fe(II) oxidation must have been larger than the occurring Fe(III) reduction. Therefore, the absolute Fe(II) oxidation rates in the high-TOC microcosms must have been considerably higher than the measured net Fe(II) oxidation rates of 12–21 $\mu M\ day^{-1}$, and were probably even higher than the measured rates for the low-TOC sediment (29–41 $\mu M\ day^{-1}$), where Fe(III) reduction is expected to play a minor role due to the lower TOC.

In summary, these results indicate (i) that we only measured net rates of Fe(II) oxidation and therefore probably underestimate Fe(II) oxidation rates by photoferrotrophs, especially in the high-TOC sediment, (ii) that there is the potential for microbial Fe-cycling in the anoxic part of the photic zone of the sediment and (iii) that microbial Fe cycling is probably more important in sediments that contain more organic carbon.

Effect of sediment organic carbon content on rates of nitrate-reducing Fe(II) oxidation and the stoichiometry of $nitrate_{reduced}$:$Fe(II)_{oxidized}$

In microcosms with high- and low-TOC sediment, we found that under conditions that favor the activity of

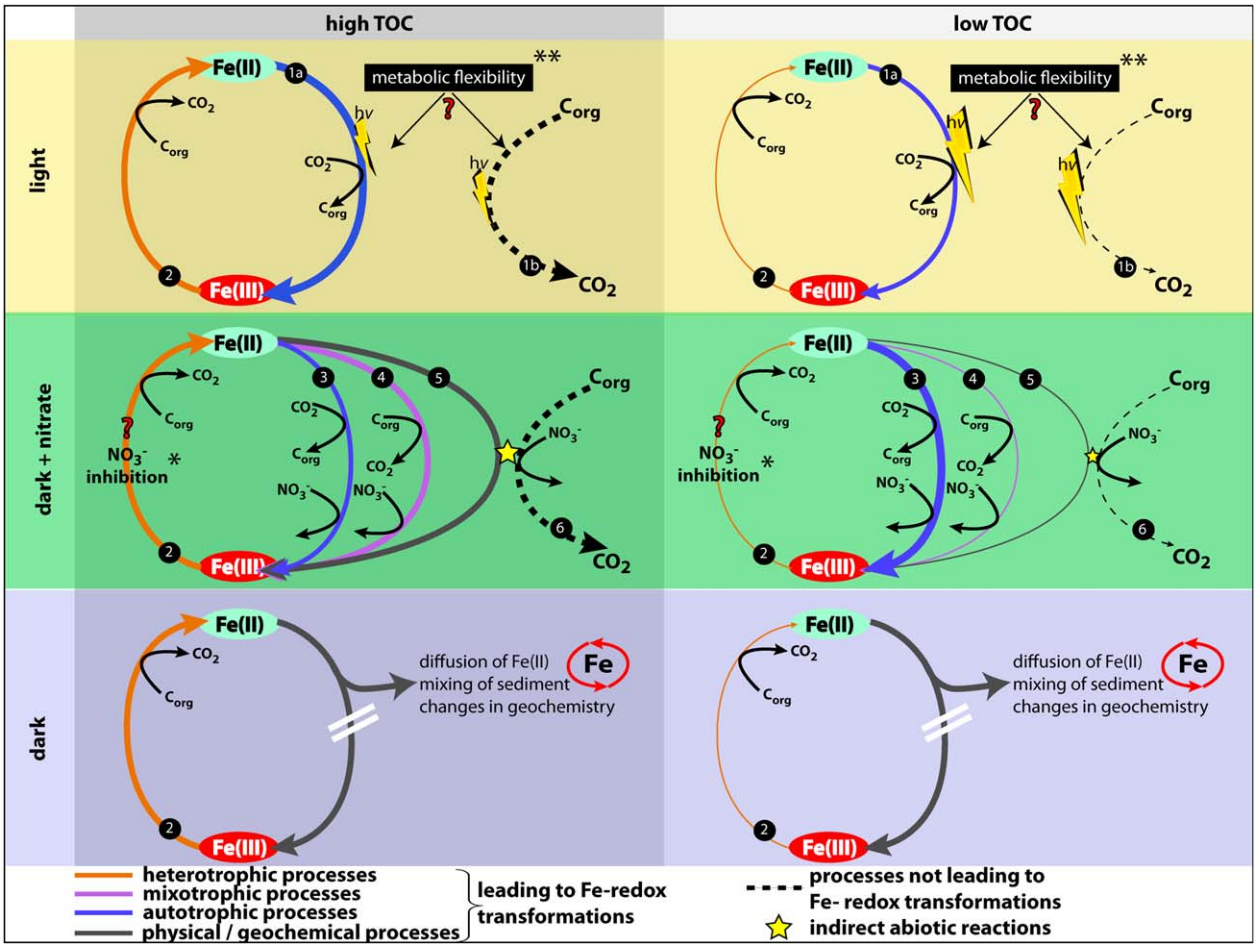

Fig. 7. Conceptual model of the influences of high-TOC and low-TOC on microbial Fe-cycling. The model is based on results of microcosm experiments with high-TOC and low-TOC sediment that was incubated in the light with addition of Fe(II) or Fe(II) and Fe(III) and in the dark with the addition of nitrate and Fe(II), or nitrate, Fe(III), and Fe(III). Thickness of lines and differences in symbol size indicate the importance of a certain process based on the experimentally determined rates. Numbers in black circles indicate the different microbial/abiotic reactions: 1a Fe(II) oxidation by photoferrotrophs; 1b Photoferrotrophs living photoheterotrophically; 2 heterotrophic Fe(III) reduction; 3 autotrophic nitrate-reducing Fe(II) oxidation; 4 mixotrophic nitrate-reducing Fe(II) oxidation; 5 Fe(II) oxidation by reactive nitrogen species produced during heterotrophic nitrate reduction; 6 heterotrophic nitrate reduction.
The asterisk indicates nitrate should inhibit Fe(III) reduction, this could however not be proven in the microcosm experiments.
The double asterisk indicates photoferrotrophs are known to be metabolically flexible, we could not show whether the photoferrotrophs were preferring Fe(II) or organic carbon in our microcosm incubations.

nitrate-reducing Fe(II)-oxidizers, Fe(II) was oxidized while nitrate was reduced and some nitrite accumulated (Figs. 2–4). Unexpectedly, we did not observe significant differences in rates of Fe(II) oxidation when comparing nitrate-reducing Fe(II) oxidation in high- and low-TOC sediments. This was surprising, because most known nitrate-reducing Fe(II)-oxidizers are mixotrophic (Muehe *et al.*, 2009; Melton *et al.*, 2014a) and we expected that the Fe(II) oxidation rates would be higher in the sediment with the higher organic carbon content. The similarity of the Fe(II) oxidation rates at different TOC contents suggests that organic carbon availability does not limit the nitrate-reducing Fe(II) oxidation and could indicate the presence of autotrophic nitrate-reducing Fe(II)-oxidizers in these sediments.

Instead of different Fe(II) oxidation rates, we found that the stoichiometry of $nitrate_{reduced}$:$Fe(II)_{oxidized}$ varied between the sediment types and the various experimental set-ups with different Fe(II) and nitrate amendments. If nitrate-reducing Fe(II)-oxidizers produce N_2 as an end product, the stoichiometry of $nitrate_{reduced}$:$Fe(II)_{oxidized}$ would result in a ratio of 0.2 for autotrophic nitrate-reducing Fe(II) oxidation. However, the measured ratios of $nitrate_{reduced}$:$Fe(II)_{oxidized}$ were all considerably higher than 0.2 with much higher values in the high-TOC compared with the low-TOC sediment. Values higher than 0.2 indicate that

more nitrate was reduced than necessary to oxidize only Fe(II), providing evidence for the occurrence of heterotrophic nitrate reduction or mixotrophic nitrate-reducing Fe(II) oxidation fueled by organic carbon present in the sediment. In the second Fe-redox cycle (following the re-addition of nitrate after the depletion of initially added nitrate and the reduction of Fe(III)), the $nitrate_{reduced}$:$Fe(II)_{oxidized}$ ratios for the high-TOC sediments were 0.9-1.6 and, thus, similar to the value of the low-TOC sediment (1.3) in the first Fe-redox cycle (Table 2). The lower $nitrate_{reduced}$:$Fe(II)_{oxidized}$ ratio in the second Fe redox cycle in the high-TOC sediment compared with the first redox cycle could be due to a decrease (consumption) of bioavailable carbon and, thus, a decreasing contribution of mixotrophic nitrate-reducing Fe(II)-oxidizers and heterotrophic nitrate-reducers.

In order to determine accurate rates of Fe(II) oxidation and the stoichiometry of $nitrate_{reduced}$:$Fe(II)_{oxidized}$, it is necessary to know whether Fe(III) reduction is occurring simultaneously with Fe(II) oxidation. Based on our current data, we cannot fully evaluate whether and/or to which extent the determined Fe(II) oxidation rates were net rates of nitrate-reducing Fe(II) oxidation or whether they were overprinted by concurrent Fe(III) reduction. From our results we conclude that microbial Fe-cycling is more active in the high TOC sediment (as indicated in Fig. 7), which shows a conceptual model of how TOC, light, and nitrate influence microbial Fe-cycling.

Conclusion

Our previous study revealed the co-existence of the different types of Fe(II)-oxidizing bacteria together with Fe(III)-reducers in sediments from Norsminde Fjord (high-TOC) and Kalø Vig (low-TOC) (Laufer *et al.*, 2016). Here we demonstrate that microbial Fe cycling occurs in these marine sediments. A conceptual model for the influences of TOC, light, and nitrate on Fe-cycling is presented in Fig. 7. The measured net phototrophic and nitrate-reducing Fe(II) oxidation rates are influenced by the concentration of bioavailable organic carbon and the resulting activities of Fe(III)-reducers. While we demonstrated that under conditions where light but no nitrate is available, Fe(II) oxidation and Fe(III) reduction can happen simultaneously, it is not clear whether Fe(II) oxidation and Fe(III) reduction are also co-occurring when nitrate is present (Fig. 7). In order to fully evaluate the importance of these processes in redox-zoned sediments in future studies, it is necessary to (i) include the contribution of microaerophilic Fe(II)-oxidizers, (ii) to consider the spatial distribution of the microorganisms involved and (iii) to take into account the gradients of electron donors, electron acceptors and light together with seasonal or daily fluctuations.

Experimental procedures

Study sites

Sediment was sampled in June 2014 and February 2015 by push-cores at two sites in the Aarhus Bay area (Denmark). Samples of organic-rich black mud were taken at 0.5 m water depth from a shallow brackish estuary, Norsminde Fjord, near its narrow entrance from Aarhus Bay (N 56° 01.171′; E 010° 15.390′). In the following, the sediment from this field site will be called high-TOC sediment. Samples of organic-poor silty-sandy sediment were taken at 0.5–1 m water depth from a beach, Kalø Vig, (N 56° 16.811′; E 010° 28.056′). In the following the sediment from this field site will be called low-TOC. The sites have mean tidal amplitude of < 20 cm.

Geochemical measurements

Sediment and pore water characteristics were measured in the field (pH, temperature, salinity and oxygen concentration of the water column, or in the laboratory (microsensor profiles of oxygen concentration, redox potential, sulfide concentration, and pH; sediment water content and TOC; pore water DOC; nitrate and nitrite). Iron speciation and concentration in the sediment and the porewater were measured as described in Laufer and colleagues (2016).

Sampling of sediment and preparation of microcosms

Sediment for microcosm incubations was sampled in coreliners with 2.5 cm inner diameter (cut-off 50 ml syringes). The uppermost 3 cm of several sediment cores was pooled and homogenized. Microcosm incubations were set up in 100 ml serum vials that were wrapped twice with aluminum foil for the dark incubations. 5 g of homogenized sediment and 50 ml seawater medium were used for each microcosm. The headspace of the microcosms was N_2/CO_2 (90:10). All preparation steps for the microcosms were undertaken in an anoxic glovebox (100% N_2 atmosphere). For preparation of the seawater medium, seawater retrieved at each site was made anoxic by flushing with N_2 for 1 h per liter, filtering it through a 0.22 μm filter (EMD Millipore Steritop^{TM}), replacing the headspace by N_2/CO_2 (90:10), adding 20 mM $NaHCO_3$ as pH buffer, and adding 1 ml l^{-1} vitamin solution (Widdel and Pfennig, 1981), 1 ml l^{-1} trace element solution (Tschech and Pfennig, 1984), and 1 ml l^{-1} selenite/tungstate solution (Widdel, 1980). To inhibit the activity of sulfate-reducing bacteria, an anoxic and sterile 1 mM Na_2MoO_4 solution was added to a final concentration of 20 mM (Sørensen, 1982; Parkes *et al.*, 1989). The pH of the medium was adjusted to 7.1 and regularly checked during the incubation. For microcosm incubations different further additives (all sterile and anoxic) were added to the seawater medium in the following concentrations and varying combinations: 2 mM Fe(II) ($FeCl_2$), 4 mM NO_3^- ($NaNO_3^-$), 160 mM NaN_3, 2 mM Fe(III) [ferrihydrite prepared according to Cornell and Schwertmann (2003)]. Microcosms were incubated in the dark, in visible light (40 W halogen light bulb), or in IR light (wavelength > 730 nm). For the IR light incubations, an IR bandpass filter (Lee infra-red filter 87, UK) was placed between the microcosms and a 40 W halogen light bulb. This was done to avoid oxygen production by oxygenic

photosynthesis in the microcosms (Trouwborst *et al*., 2007; Wilbanks *et al*., 2014). All incubations were at 20°C.

In June 2014, the following microcosms were prepared in triplicates: With high-TOC sediment microcosms (i) without additives in the light, (ii) with Fe(II) in the light, (ii) with NO_3^- in the dark, (iv) with Fe(II) and NO_3^- in the dark and (5) controls of all these setups to which additionally NaN_3 was added to inhibit microbial respiration. The efficiency of the NaN_3 inhibition was evaluated with several enrichment/pure cultures of nitrate-reducing Fe(II)-oxidizers, photoferrotrophs and Fe(III) reducers at different concentrations of NaN_3 (1–160 mM). No Fe(II) oxidation or Fe(III) reduction was detected in these tests (data not shown). The parameters measured in these microcosms were: (a) cell numbers of Fe-metabolizing microorganisms by the MPN method in the beginning and the end of the incubation, (b) changes of Fe(II) and Fe(III) concentrations in bulk (extraction with 40 mM sulfamic acid) and in the dissolved phase, (c) concentrations of NO_3^- and NO_2^-, (d) DOC, and (e) VFA) concentrations, all measured over time of incubation. All measurements were performed for each of the triplicate microcosms. Because a large volume of sample was needed for all analyses, several sets of triplicates were prepared (in total 21 microcosms of each incubation condition). Measurements of Fe(II), Fe(III), NO_3^- and NO_2^- were always carried out in the same triplicate set until the whole content of the microcosms was sampled for DOC and VFA measurements. A second set of triplicates, that had been incubated under the same conditions as the first set, was used for continued measurements. After 47 days, NO_3^- or ferrihydrite was added again to some of the microcosms that were incubated in the dark with NO_3^- or with NO_3^- and Fe(II). After 69 days, some of the previously light incubated microcosms were placed in the dark.

With the low-TOC sediment from June 2014, the following microcosms were prepared in triplicates: (i) medium containing Fe(II) incubated in light, (ii) medium containing Fe(II) and NO_3^- incubated in the dark and (iii) controls of all these setups to which additionally NaN_3 was added. The parameters measured in these microcosms were: (a) changes of Fe(II) and Fe(III) concentrations in total and dissolved phase over time of incubation, (b) concentrations of NO_3^- and NO_2^- over time of incubation, and (c) DOC in the beginning and the end of incubation.

In February 2015 the following microcosms were prepared in triplicates: With the high-TOC sediment (i) microcosms with Fe(II) and Fe(III) incubated in light, (ii) with Fe(II), Fe(III), and NO_3^- and (iii) controls of all these setups to which additionally NaN_3 was added. The parameters measured in these microcosms were: (a) changes of concentrations of Fe(II) and Fe(III) in the total and dissolved phase over time of incubation, (b) concentrations of NO_3^- and NO_2^- over time of incubation. All parameters were measured in triplicate microcosms. Additionally, microcosms with high-TOC and low-TOC sediment were set up to test for oxygenic photosynthesis. Therefore, Fe(II) was added to two sets of triplicate microcosms from each site and one set of triplicates was incubated in normal light, and one in IR light. Additionally, inhibited controls were prepared by adding NaN_3. In these set-ups only the concentrations of Fe(II) and Fe(III) in total and dissolved phase were measured over the time of the incubation.

Analytical methods for microcosm experiments

Iron, nitrate and nitrite concentrations in microcosms. For measuring Fe(II) and total Fe, 1 ml of slurry from each microcosm was sampled with a syringe and a thick needle (1.2 x 40 mm) inside an anoxic glovebox (100% N_2 atmosphere). Hundred microlitre of this slurry sample was added to 900 μl sulfamic acid (40 mM) and placed on a shaker (150 rpm) for 1 h. The samples were then centrifuged (5 min, 7000 g, Eppendorf 5430R) and the supernatant was used for Fe(II) and total Fe determination with the spectrophotometric ferrozine assay (Stookey, 1970), adapted according to Klueglein and Kappler (2012). The Fe-extraction with sulfamic acid (40 mM) was developed by Klueglein and Kappler (2012) and avoids the abiotic oxidation of Fe(II) by NO_2^- during the acidic Fe-extraction. The remaining part of the initial 1 ml sample of the slurry was centrifuged (5 min, 7000 g, Eppendorf 5430R) and the supernatant was used for measurements of the dissolved phases. For dissolved Fe(II) and total Fe, 100 μl of the supernatant was added to 40 mM sulfamic acid. For NO_3^- and NO_2^-, 100 μl of the supernatant was added to 900 μl Milli-Q H_2O and stored anoxically at 4°C until analysis. Fe(II) and total Fe concentrations were determined by ferrozine assay. Concentrations of NO_3^- and NO_2^- were measured by flow injection analysis (FIA), as described by Laufer and colleagues (2016).

Calculation of maximum rates and stoichiometries of $nitrate_{reduced}$*:*$iron(II)_{oxidized}$. Rates of Fe(II) oxidation, Fe(III) reduction, and NO_3^- reduction were calculated by applying a linear regression to the measured concentrations of the respective compound over time of incubation at the steepest part of increasing or decreasing concentrations. At least three time points were used for each rate calculation. The stoichiometries of $nitrate_{reduced}$:$iron(II)_{oxidized}$ at different time intervals were calculated by dividing the amount of nitrate (in μmol) that was reduced during that time interval (calculated from the decrease in nitrate concentrations) by the amount of Fe(II) (in μmol) that was oxidized during that time interval (calculated from the decrease in Fe(II) concentrations).

Analysis of DOC. For analysis of DOC in microcosm incubations, 20 ml of sample was necessary. Therefore, the whole microcosm content was sampled and centrifuged (15 min at 5000 g, Hermle 7300, Germany). Afterwards, the supernatant was filtered through a 0.45 μm filter (MF-Millipore MCE membrane) and the DOC concentration was measured with a carbon analyser (high TOC, Elementar, Germany).

Analysis of VFAs by 2D-IC-MS. For the measurement of VFAs, the same samples were used as for DOC measurements. After centrifugation, 3 ml of the unfiltered supernatant was sampled and placed in organic-free GC vials (burned for 5 h at 450°C), closed with screw-caps with a PTFE inlet and frozen at −80°C. Prior to the analysis, the samples were thawed and filtered through disposable syringe filters (Acrodisc® IC grade, 0.2 μm pore size, 13 mm diameter). The syringe filters were cleaned by rinsing with 10 ml of Milli-Q® water (Ultrapure, Type I) directly before use. The first 0.5 ml of filtered sample was discarded and the next 0.5 ml was used for VFA analysis. All samples were measured undiluted. Samples with high acetate concentrations (above 100 μM) were additionally measured after 1:10 dilution with Milli-Q water. VFAs were measured by 2-dimensional ion chromatography-

mass spectrometry (2D IC-MS), as described in detail in Glombitza and colleagues (2014) using a dual Dionex ICS3000 ion chromatograph coupled to an MSQ Plus mass spectrometer (Thermo Scientific). By this method the first IC dimension is used to separate the bulk VFAs from the inorganic ions of the sample matrix (i.e. the incubation medium). The VFAs are trapped on a concentrator column (Dionex IonPac™ UTAC-ULP1, Thermo Scientific) and subsequently separated in the second IC dimension. The column for the first dimension was a Dionex IonPac™ AS24, and for the second dimension a Dionex IonPac™ AS11HC (both, Thermo Scientific). Detection limits for the individual VFAs were between 0.1 and 0.5 μM. For a detailed discussion of analytical and statistical parameters (detection limits, sensitivity, accuracy and precision) see Glombitza and colleagues 2014. Iso-butyrate was not described in Glombitza and colleagues 2014, but the statistical analytical parameters (limit of detection, sensitivity, accuracy and precision) were determined in the present study by measurements of 15 replicates of a low concentration iso-butyrate standard (100 ppb = 1.15 μM) and found to be the same as for butyrate.

Analysis of mineralogy by Mössbauer spectroscopy

Samples for Mössbauer measurements were taken from a sediment slurry without any amendments (just containing the homogenized sediment and the anoxic seawater medium). In an anoxic glovebox (100% N_2 atmosphere) samples were passed through filters (0.45 μm, cellulose acetate, Millipore) which were then sealed between two layers of air-tight Kapton tape and frozen under anoxic conditions at −20°C until each measurement could be carried out. Samples were measured at low temperature in a He atmosphere to prevent abiotic oxidation. They were individually loaded into the cryostat and measured at 77 K and at 5 K. The spectrometer (WissEL) was operated in transmission mode, with a ^{57}Co/Rh source driven in constant acceleration mode and calibrated with a 7 μm thick α ^{57}Fe foil measured at room temperature. Spectra were fitted using the Voigt based fitting method using the Recoil software (Rancourt and Ping, 1991), with the half width at half maximum set to ∼0.138 mm s^{-1} during fitting. Each sample took between 2 and 3 days to measure.

Determination of cell numbers of the different iron-metabolizers by MPNs

Enumeration of Fe-metabolizing microorganisms in June 2014 and February 2015 was done for the original sediment used for inoculation of the microcosms (homogenized sediment from sediment cores, 0–3 cm sediment depth) and from microcosms with high-TOC sediment from June 2014 after 100 days of incubation. Viable cell numbers of autotrophic nitrate-reducing Fe(II)-oxidizers, mixotrophic nitrate-reducing Fe(II)-oxidizers, photoferrotrophs (in IR light), and Fe(III)-reducing bacteria were determined according to the MPN method and with artificial seawater medium (ASW) as described in Laufer and colleagues (2016).

Acknowledgements

We thank Ellen Struve for support with geochemical measurements, Jeanette Pedersen for help with sampling porewater from sediment cores and VFA measurements. Furthermore, we thank Chihiro Murata for help with ferrozine assays. This project was supported by the European Research Council under the European Union's Seventh Framework Program (FP/2007–2013)/ERC Grant, agreement no. 307320-MICROFOX. CG was funded by a Marie-Curie Individual Fellowship, IEF (EU FP7, agreement no. 327675-DEEP CARBON FLUX). BBJ was funded by the Danish National Research Foundation (Grant No. DNRF104) and by ERC Advanced Grant (Grant No. 294200-MICROENERGY).

References

Ansbaek, J., and Blackburn, T.H. (1980) A method for the analysis of acetate turnover in a coastal marine sediment. *Microb Ecol* **5:** 253–264.

Benz, M., Brune, A., and Schink, B. (1998) Anaerobic and aerobic oxidation of ferrous iron at neutral ph by chemoheterotrophic nitrate-reducing bacteria. *Arch Microbiol* **169:** 159–165.

Benzine, J., Shelobolina, E., Xiong, M.Y., Kennedy, D.W., McKinley, J.P., Lin, X., and Roden, E.E. (2013) Fe-phyllosilicate redox cycling organisms from a redox transition zone in Hanford 300 Area sediments. *Front Microbiol* **4:** 1–13.

Boyd, P.W., Jickells, T., Law, C., Blain, S., Boyle, E., Buesseler, K., *et al.* (2007) Mesoscale iron enrichment experiments 1993-2005: synthesis and future directions. *Science* **315:** 612–617.

Byrne, J.M., Klueglein, N., Pearce, C., Rosso, K.M., Appel, E., and Kappler, A. (2015) Redox cycling of Fe(II) and Fe(III) in magnetite by Fe-metabolizing bacteria. *Science* **347:** 1473–1476.

Caccavo, F., Blakemore, R.P., and Lovley, D.R. (1992) A hydrogen-oxidizing, Fe (III)-reducing microorganism from the great bay estuary, New Hampshire. *Appl Environ Microbiol* **58:** 3211–3216.

Canfield, D.E. (1989) Reactive iron in marine sediments. *Geochim Cosmochim Acta* **53:** 619–632.

Canfield, D.E., Jørgensen, B.B., Fossing, H., Glud, R., Gundersen, J., Ramsing, N.B., *et al.* (1993a) Pathways of organic carbon oxidation in three continental margin sediments. *Marine Geol* **113:** 27–40.

Canfield, D.E., Thamdrup, B., and Hansen, J.W. (1993b) The anaerobic degradation of organic matter in Danish coastal sediments: Iron reduction, manganese reduction, and sulfate reduction. *Geochim Cosmochim Acta* **57:** 3867–3883.

Carlson, H.K., Clark, I.C., Blazewicz, S.J., Iavarone, A.T., and Coates, J.D. (2013) Fe(II) oxidation is an innate capability of nitrate-reducing bacteria that involves abiotic and biotic reactions. *J Bacteriol* **195:** 3260–3268.

Chakraborty, A., and Picardal, F. (2013) Induction of nitrate-dependent Fe(II) oxidation by Fe(II) in *Dechloromonas* sp. strain UWNR4 and *Acidovorax* sp. strain 2AN. *Appl Environ Microbiol* **79:** 748–752.

Chakraborty, A., Roden, E.E., Schieber, J., and Picardal, F. (2011) Enhanced growth of *Acidovorax* sp. strain 2AN

during nitrate-dependent Fe(II) oxidation in batch and continuous-flow systems. *Appl Environ Microbiol* **77:** 8548–8556.

Christensen, D., and Blackburn, T. (1982) Turnover of ^{14}C-labelled acetate in marine sediments. *Mar Biol* **71:** 113–119.

Coby, A.J., Picardal, F., Shelobolina, E., Xu, H. and Roden, E.E. (2011) Repeated anaerobic microbial redox cycling of iron. *Appl Environm Microbiol* **77:** 6036–6042.

Cornell, R.M., and Schwertmann, U. (2003) The Iron Oxides: Structure, Properties, Reactions, *Occurrences and Uses*. John Willey & Sons, Weinheim.

D'Hondt, S., Jørgensen, B.B., Miller, D.J., Batzke, A., Blake, R., Cragg, B.A., et al. (2004) Distributions of microbial activities in deep subseafloor sediments. *Science* **306:** 2216–2221.

Ehrenreich, A., and Widdel, F. (1994) Anaerobic oxidation of ferrous iron by purple bacteria, a new type of phototrophic metabolism. *Appl Environ Microbiol* **60:** 4517–4526.

Emerson, D., and Moyer, C. (1997) Isolation and characterization of novel iron-oxidizing bacteria that grow at circumneutral pH. *Appl Environ Microbiol* **63:** 4784–4792.

Finke, N., Vandieken V., and Jørgensen, B.B. (2007) Acetate, lactate, propionate, and isobutyrate as electron donors for iron and sulfate reduction in arctic marine sediments, Svalbard. *FEMS Microbiol Ecol* **59:** 10–22.

Fuchs, G. (2007). *Allgemeine Mikrobiologie. Verlag: Georg Thieme*, pp. 347–378.

Fukui, M., Suh, J., Yonezawa, Y., and Urushigawa, Y. (1997) Major substrates for microbial sulfate reduction in the sediments of Ise Bay, Japan. *Ecol Res* **12:** 201–209.

Gibson, G., Parkes, R., and Herbert, R. (1989) Biological availability and turnover rate of acetate in marine and estuarine sediments in relation to dissimilatory sulphate reduction. *FEMS Microbiol Lett* **62:** 303–306.

Glombitza, C., Jaussi, M., Røy, H., Seidenkrantz, M.-S., Lomstein, B.A., and Jørgensen, B.B. (2015) Formate, acetate, and propionate as substrates for sulfate reduction in sub-arctic sediments of southwest Greenland. *Front Microbiol* **6:** 846. doi: 10.3389/fmicb.2015.00846.

Glombitza, C., Pedersen, J., Røy, H., and Jørgensen, B.B. (2014) Direct analysis of volatile fatty acids in marine sediment porewater by two-dimensional ion chromatography-mass spectrometry. *Limnol Oceanogr Methods* **12:** 455–468.

Haese, R.R. (2006) The biogeochemistry of iron. In *Marine Geochemistry.* Schulz, H., and Zabel, M. Berlin Heidelberg: Springer, pp. 241–270.

Harper, S.R., and Pohland, F.G. (1986) Recent developments in hydrogen management during anaerobic biological wastewater treatment. *Biotechnol Bioeng* **28:** 585–602.

Jones, J.G., Gardener, S., and Simon, B.M. (1983) Bacterial reduction of ferric iron in a stratified eutrophic lake. *J Gen Microbiol* **129:** 131–139.

Klueglein, N., and Kappler, A. (2012) Abiotic oxidation of Fe(II) by reactive nitrogen species in cultures of the nitrate-reducing Fe(II) oxidizer *Acidovorax* sp. BoFeN1 - questioning the existence of enzymatic Fe(II) oxidation. *Geobiology* **11:** 180–190.

Klueglein, N., Picardal, F., Zedda, M., Zwiener, C. and Kappler, A. (2015). Oxidation of Fe (II)-EDTA by nitrite and by two nitrate-reducing Fe (II)-oxidizing *Acidovorax* strains. *Geobiology* **13:** 198–207.

Klueglein, N., Zeitvogel, F., Stierhof, Y.-D., Floetenmeyer, M., Konhauser, K. O., Kappler, A., and Obst, M. (2014) Potential role of nitrite for abiotic Fe(II) oxidation and cell encrustation during nitrate reduction by denitrifying bacteria. *Appl Environ Microbiol* **80:** 1051–1061.

Kopf, S., and Newman, D. (2012) Photomixotrophic growth of *Rhodobacter capsulatus* SB1003 on ferrous iron. *Geobiology* **10:** 216–222.

Laufer, K., Nordhoff, M., Røy, H., Schmidt, C., Behrens, S., Jørgensen, B.B. and Kappler, A. (2016) Co-existence of microaerophilic, nitrate-reducing, and phototrophic Fe(II)-oxidizers and Fe(III)-reducers in coastal marine sediment. *Appl Environ Microbiol* **82:** 1433–1447.

Lovley, D.R. (1991) Dissimilatory Fe(III) and MN(IV) reduction. *Microbiol Rev* **55:** 259–287.

Lovley, D.R., and Phillips, E.J. (1989) Requirement for a microbial consortium to completely oxidize glucose in Fe(II)-reducing sediments. *Appl Environ Microbiol* **55:** 3234–3236.

Lovley, D.R., Phillips, E., Lonergan, D.J., and Widman, P.K. (1995) Fe(Fe(III)) and S(0) reduction by *Pelobacter carbinolicus*. *Appl Environ Microbiol* **61:** 2132–2138.

Martin, J.H. Gordon, M., and Fitzwater, S.E. (1991) The case for iron. *Limnol Oceanogr* **36:** 1793–1802.

Melton, E.D., Schmidt, C., and Kappler, A. (2012) Microbial iron(II) oxidation in littoral freshwater lake sediment: The potential for competition between phototrophic vs. nitrate-reducing iron(II)-oxidizers. *Front Microbiol* **3:** 197.

Melton, E.D., Schmidt, C., Behrens, S., Schink, B. and Kappler, A. (2014) Metabolic flexibility and substrate preference by the Fe (II)-oxidizing purple non-sulphur bacterium Rhodopseudomonas palustris strain TIE-1. *Geomicrobiology Journal* 31, 835–843.

Melton, E.D., Swanner, E.D., Behrens, S., Schmidt, C., and Kappler, A. (2014a) The interplay of microbially mediated and abiotic reactions in the biogeochemical Fe cycle. *Nat Rev Microbiol* 12: 797–808.

Melton, E., Schmidt, C., Behrens, S., Schink, B., and Kappler, A. (2014b) Metabolic flexibility and substrate preference by the Fe(II)-oxidizing purple non-sulphur bacterium *Rhodopseudomonas palustris* strain TIE-1. *Geomicrobiol J* **31:** 835–843.

Moeslund, L., Thamdrup, B., and Jørgensen, B.B. (1994) Sulfur and iron cycling in a coastal sediment: Radiotracer studies and seasonal dynamics. *Biogeochemistry* **27:** 129–152.

Muehe, E.M., Gerhardt, S., Schink, B., and Kappler, A. (2009) Ecophysiology and the energetic benefit of mixotrophic Fe(II) oxidation by various strains of nitrate-reducing bacteria. *FEMS Microbiol Ecol* **70:** 335–343.

Murad, E., and Cashion, J. (2004) *Mössbauer Spectroscopy of Environmental Materials and Their Industrial Utilization*. Kluwer Academic Publishers, New York.

Oremland, R., and Capone, D. (1988) Use of "specific" inhibitors in biogeochemistry and microbial ecology. In *Advances in Microbial Ecology.* Marshall, K.C., (eds). Springer, Boston, MA, pp. 285–383.

Parkes, R.J., Taylor, J., and Jørck-Ramberg, D. (1984) Demonstration, using *Desulfobacter* sp., of two pools of acetate with different biological availabilities in marine pore water. *Mar Biol* **83:** 271–276.

Parkes, R., Gibson, G., Mueller-Harvey, I., Buckingham, W., and Herbert, R. (1989) Determination of the substrates for sulphate-reducing bacteria within marine and esturaine sediments with different rates of sulphate reduction. *J Gen Microbiol* **135:** 175–187.

Rancourt, D., and Ping, J. (1991) Voigt-based methods for arbitrary-shape static hyperfine parameter distributions in Mössbauer spectroscopy. *Nucl Instrum Methods Phys Res B* **58:** 85–97.

Rossello-Mora, R.A., Caccavo F., Jr, Osterlehner, K., Springer, N., Spring, S., Schüler, D., *et al*. (1995) Isolation and taxonomic characterization of a halotolerant, facultatively iron-reducing bacterium. *Syst Appl Microbiol* **17:** 569–573.

Schink, B. (1997) Energetics of syntrophic cooperation in methanogenic degradation. *Microbiol Mol Biol Rev* **61:** 262–280.

Schink, B., and Stams, A.J. (2013) *Syntrophism Among Prokaryotes*. Berlin: Springer.

Shelobolina, E., Konishi, H., Xu, H., Benzine, J., Xiong, M.Y., Wu, T., *et al*. (2012) Isolation of phyllosilicate–iron redox cycling microorganisms from an illite–smectite rich hydromorphic soil. *Front Microbiol* **3:** 1–10.

Sørensen, J. (1982) Reduction of ferric iron in anaerobic, marine sediment and interaction with reduction of nitrate and sulfate. *Appl Environ Microbiol* **43:** 319–324.

Sørensen, J., Christensen, D., and Jørgensen, B.B. (1981) Volatile fatty acids and hydrogen as substrates for sulfate-reducing bacteria in anaerobic marine sediment. *Appl Environ Microbiol* **42:** 5–11.

Stookey, L.L. (1970) Ferrozine—*a new spectrophotometric reagent for iron. Anal Chem* **42:** 779–781.

Straub, K.L., Benz, M., Schink, B., and Widdel, F. (1996) Anaerobic, nitrate-dependent microbial oxidation of ferrous iron. *Appl Environ Microbiol* **62:** 1458–1460.

Straub, K.L., Hanzlik, M., and Buchholz-Cleven, B.E. (1998) The use of biologically produced ferrihydrite for the isolation of novel iron-reducing bacteria. *Syst Appl Microbiol* **21:** 442–449.

Straub, K.L., Schonhuber, W.A., Buchholz-Cleven, B.E.E., and Schink, B. (2004) Diversity of ferrous iron-oxidizing, nitrate-reducing bacteria and their involvement in oxygen-independent iron cycling. *Geomicrobiol J* **21:** 371–378.

Thamdrup, B. (2000) Bacterial manganese and iron reduction in aquatic sediments. In *Advances in Microbial Ecology*. Schink, B. (ed.), New York: Kluwer Academic/Plenum Publishers, pp. 41–84.

Thamdrup, B., Fossing, H., and Jørgensen, B.B. (1994) Manganese, iron and sulfur cycling in a coastal marine sediment, Aarhus Bay, Denmark. *Geochim Cosmochim Acta* **58:** 5115–5129.

Trouwborst, R.E., Johnston, A., Koch, G., Luther Iii, G.W., and Pierson, B.K. (2007) Biogeochemistry of Fe(II) oxidation in a photosynthetic microbial mat: implications for precambrian Fe(II) oxidation. *Geochim Cosmochim Acta* **71:** 4629–4643.

Tschech, A., and Pfennig, N. (1984) Growth yield increase linked to caffeate reduction in *Acetobacterium woodii*. *Arch Microbiol* **137:** 163–167.

Tugel, J.B., Hines, M.E., and Jones, G.E. (1986) Microbial iron reduction by enrichment cultures isolated from estuarine sediments. *Appl Environ Microbiol* **52:** 1167–1172.

Weber, K.A., Achenbach, L.A., and Coates, J.D. (2006a) Microorganisms pumping iron: anaerobic microbial iron oxidation and reduction. *Nat Rev Microbiol* **4:** 752–764.

Weber, K.A., Urrutia, M.M., Churchill, P.F., Kukkadapu, R.K., and Roden, E.E. (2006b) Anaerobic redox cycling of iron by freshwater sediment microorganisms. *Environ Microbiol* **8:** 100–113.

Widdel, F. (1980) Anaerober Abbau von Fettsäuren und Benzoesäure durch neu isolierte Arten Sufat reduzierender Bakterien. Dissertation Thesis, Universität Göttingen.

Widdel, F., and Pfennig, N. (1981) Studies on dissimilatory sulfate-reducing bacteria that compose fatty acids- *i. Isolation of a new sulfate-reducer enriched with acetate from saline enviroments. Description of Desulfobacter postgatei gen. nov. sp. nov. Arch Microbiol* **129:** 395–400.

Widdel, F., Schnell, S., Heising, S., Ehrenreich, A., Assmus, B., and Schink, B. (1993) Ferrous iron oxidation by anoxygenic phototrophic bacteria. *Nature* **362:** 834–836.

Wilbanks, E.G., Jaekel, U., Salman, V., Humphrey, P.T., Eisen, J.A., Facciotti, M.T., *et al*. (2014) Microscale sulfur cycling in the phototrophic pink berry consortia of the Sippewissett salt marsh. *Environ Microbiol* **16:** 3398–3415.

Wilson, D.F., and Chance, B. (1967) Azide inhibition of mitochondrial electron transport i. The aerobic steady state of succinate oxidation. *Biochim Biophys Acta* **131:** 421–430.

Supporting information

Additional Supporting Information may be found in the online version of this article at the publisher's web-site:

Fig. S1. Fe data of microcosms for determination of photoferrotrophic Fe(II)-oxidation rates incubated in "normal" light (NL) and in infra-red light (IR). Controls were treated with NaN_3. Error bars indicate standard deviation.

Fig. S2. Data of VFA measurements from microcosms with the high-TOC sediment from June 2014. A: in microcosms that were incubated in the light w/o further additives. B: microcosms that were incubated in the light to which 2 mM Fe(II) were added. C: microcosms that were incubated in the light w/o further additives and were shifted from light to dark incubation after 69 days. D: microcosms that were incubated in the light to which 2 mM of Fe(II) were added and were shifted from light to dark incubation after 69 days. E: microcosms that were incubated in the dark to which only nitrate was added. F: microcosms that were incubated in the dark to which nitrate and Fe(II) were added. G: microcosms that were incubated in the dark to which initially only nitrate was added and after 49 days Fe(III) was added. H: microcosms that were incubated in the dark to which initially nitrate and Fe(II) were added and after 49 days Fe(III) was added. I: microcosms that were incubated in the dark w/o any additives. J: mean of all microcosms that were treated with NaN_3.

Fig. S3. Mössbauer spectra of starting Norsminde Fjord sediments without any amendments collected at (a) 77 K and (b) 5 K.

Table S1. MPN numbers of original sediment from the high (Norsminde Fjord)- and low-TOC (Kalø Vig) sediment.

Table S2. Fitting parameters of Norsminde Fjord starting recorded at 5 K and 77 K.